Effectiveness and Predictability of Particle Damping

Bryce L. Fowler, Eric M. Flint
CSA Engineering, Inc.
2565 Leghorn Street
Mountain View, CA 94043

Steven E. Olson
University of Dayton Research Institute
300 College Park
Dayton, OH 45469

Effectiveness and Predictability of Particle Damping

Bryce L. Fowler[a], Eric M. Flint[a], Steven E. Olson[b]

[a] CSA Engineering, Inc., 2565 Leghorn Street, Mountain View, CA 94043
[b] University of Dayton Research Institute, 300 College Park, Dayton, OH 45469

ABSTRACT

In this paper, recent results of ongoing studies into the effectiveness and predictability of particle damping are discussed. Efforts have concentrated on characterizing and predicting the behavior of a wide range of potential particle materials, shapes, and sizes in the laboratory environment, as well as at elevated temperature. Methodologies used to generate data and extract the characteristics of the nonlinear damping phenomena are illustrated with interesting test results. Experimental results are compared to predictions from analytical simulations performed with an explicit code, based on the particle dynamics method, that has been developed in support of this work.

Keywords: Nonlinear, Particle, Granular, Impact, Damping

1. INTRODUCTION

Particle damping is a derivative of impact damping where multiple auxiliary masses of small size are placed inside a cavity attached to the vibrating structure. Particle damping can perform at elevated temperatures where most other forms of passive damping cannot. Studies conducted over recent years have demonstrated the effectiveness and potential application of particle dampers, and have shown that particle dampers are highly nonlinear dampers whose energy dissipation, or damping, is derived from a combination of loss mechanisms. The relative effectiveness of these mechanisms changes based on various system parameters. Due to the complex interactions involved in the particle damper, a comprehensive design methodology has not been developed which will allow particle damping technology to be implemented without extensive trial-and-error testing. Development of a design methodology for the implementation of particle damping is the goal of the present effort. Results from analytical modeling and experimental testing efforts are presented.

2. MODELING PARTICLE DAMPING

The particle damper is conceptually a relatively simple device. However, the behavior of the particle damper is highly nonlinear and energy dissipation, or damping, is derived from a combination of loss mechanisms. The relative effectiveness of these mechanisms changes based on various system parameters. In the following paragraphs, the loss mechanisms present in the particle damper are reviewed, along with the incorporation of these loss mechanisms into a mathematical model.

Passive damping techniques attenuate the response of a vibrating structure by removing a portion of the vibratory energy. One method of removing the vibratory energy is to transfer the energy to a secondary system. Dynamic vibration absorbers function in this manner. Oscillations of the dynamic vibration absorber are created with a fraction of the energy creating the oscillations of the primary system. This mechanism is present in the particle damper in the form of the momentum transfer which occurs when the particles impact the cavity walls.

A second method of removing the vibratory energy is to dissipate the mechanical energy in the form of heat or noise. Viscoelastic and viscous damping dissipate energy in the form of heat created when the viscoelastic or viscous fluid undergoes shear. Friction damping also dissipates energy in the form of heat which is created due to the relative motion between two contacting surfaces. In particle dampers, friction exists when relative sliding (or, to a much lesser degree, rolling) motion occurs between individual particles in contact or between particles in contact with the cavity walls. Viscoelastic behavior also is present in the particle dampers due to impacts with non-unity coefficients of restitution (i.e., impacts which are not perfectly elastic).

For convenience, the loss mechanisms present in the particle damper can be grouped into "external" and "internal" mechanisms. External mechanisms involve friction and impact interactions between the particles and the cavity. Internal mechanisms involve friction and impact interactions between the individual particles. The relative effectiveness of these mechanisms changes based on various system parameters. For example, at low excitation levels or for relatively long cavity lengths, insufficient energy may exist to create impacts between the particles and the cavity ends. Under such circumstances,

any dissipation would be due solely to any sliding or rolling friction between the particles and the cavity or interactions between the individual particles. For higher excitations or shorter cavity lengths, however, losses due to impacts between the particles and cavity ends may dominate the overall dissipation.

Earlier particle damper modeling efforts have included the use of a single mass to simulate the particles [1-5]. These models appear to provide a reasonable approximation of the external friction and impact interactions between the particle and the cavity. However, these models do not provide a suitable means to model internal friction and impact interactions between the individual particles. As a result, attention was focused on alternative modeling techniques with the potential to capture both external and internal mechanisms.

Recently, Salueña, *et al.* [6] have performed limited studies to mathematically evaluate the dissipative properties of granular materials using the particle dynamics method. The particle dynamics method is a technique where individual particles are modeled and their motions tracked in time. This technique is similar to that used for modeling molecular dynamics and is useful for considering effects such as surface friction, collisional energy losses, boundary forces, and gravity. Much of the pioneering work using the particle dynamics method to simulate the behavior of granular materials was performed by Cundall and Strack [7-10]. The procedure is an explicit process with sufficiently small time steps taken such that during a single time step disturbances cannot propagate from any particle further than its immediate neighbors. As a result, at a given time, the resultant forces on any particle are determined exclusively by its interaction with the particles with which it is in contact. This feature makes it possible to follow the nonlinear interaction of a large number of particles without excessive memory or the need for an iterative procedure.

The utility of the particle dynamics method is based on the ability to simulate contact interactions based on a small number of parameters that capture the most important contact properties. Interaction forces between the individual particles and the cavity walls are calculated based on force-displacement relations. One of the critical aspects for developing an accurate mathematical model is the selection of appropriate force-displacement relations to account for the forces created due to particle-particle impacts and due to particle-cavity impacts.

For simplicity, initially it has been assumed that all particles are identical. The particles are assumed to be spherical in shape with a given radius and material properties. Consider a typical impact for two spherical particles, i and j, with radii R_i and R_j, with the particle centers separated by a distance, d_{ij}, as shown in Figure 1.
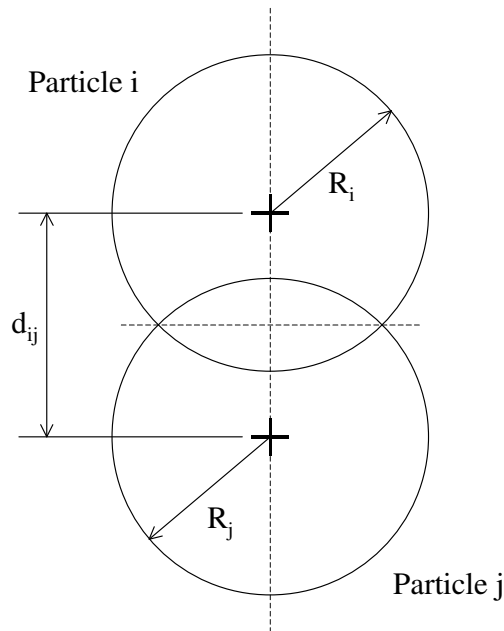

Figure 1: Typical particle-particle impact parameters

These two particles interact if their approach, α, is positive. The approach can be defined according to the following equation:

$$\alpha = \left(R_i + R_j\right) - d_{ij} \tag{1}$$

In this case, the colliding spheres feel the force:

$$\vec{F} = F^N \cdot \vec{n}^N + F^S \cdot \vec{n}^S \tag{2}$$

where F^N and F^S are the normal and shear forces, and $\vec{n}^N$ and $\vec{n}^S$ are the unit vectors in the normal and shear directions, respectively

For the normal force-displacement relations, it is necessary to consider both elastic and dissipative portions of the normal force. Lee and Radok [11] showed that, as long as the contact area is increasing, a simple relation for the total normal force can be derived by replacing the elastic modulus in Hertz's relation with the relaxation modulus of the sphere material. The total normal force (i.e., the normal force due to the combined elastic and dissipative components) at any time can be expressed as:

$$F^N(t) = \frac{2}{3R} \frac{1}{\left(1 - v^2\right)} \int_0^t \psi(t - t') \frac{d}{dt'} a(t')^3 \, dt' \tag{3}$$

where:

$$R = \frac{\left(R_i \cdot R_j\right)}{\left(R_i + R_j\right)} \tag{4}$$

and the contact circle radius, a, is related to the approach as:

$$\alpha = \frac{a^2}{R} \tag{5}$$

These equations break down when the loading history causes the contact area to decrease. The breakdown results due to unrealistic negative contact pressures which are predicted within the contact area. Ting [12-13] found that when the contact area is decreasing the impact could be described by a pair of coupled integro-differential equations for the approach and the total normal force. However, these equations must be evaluated numerically step by step. The entire loading history must be stored and the number of required function evaluations is constantly increasing during the unloading. As a result, this technique requires considerable memory and computational resources.

An alternative approach which greatly reduce the required resources is to calculate the total normal force using Lee and Radok's relation with the assumption that the total contact force goes to zero when negative forces are predicted. As shown in the load and displacement curves in Figure 2, the viscoelastic behavior calculated using this method has been shown to compare reasonably well with that predicted from ABAQUS finite element analyses.
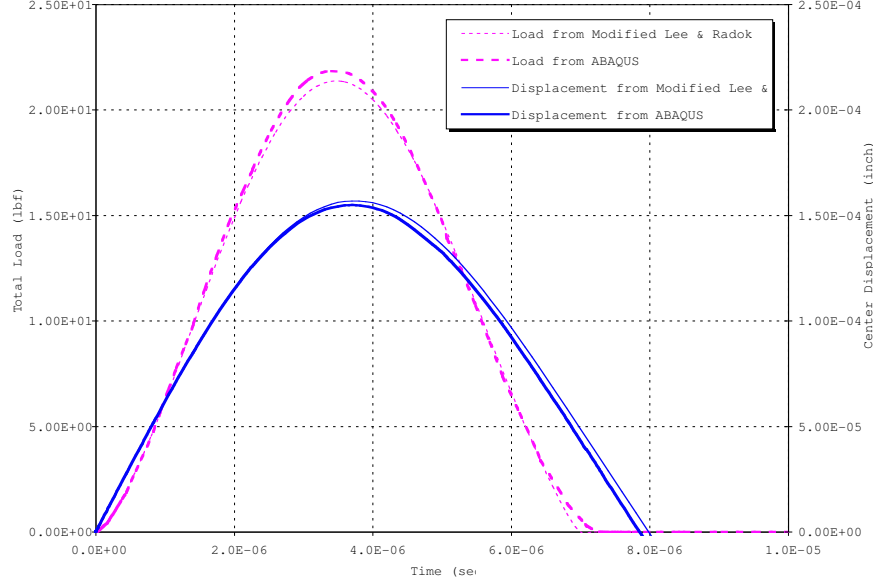
Figure 2: Comparison of viscoelastic behavior during impact

The normal forces are calculated using an incremental form of the modified Lee and Radok relation. The particles can be given elastic or viscoelastic material properties. For elastic properties, the normal force-displacement relation reverts to an incremental form of Hertz's law. Viscoelastic material properties are given as a three-parameter Maxwell model. The incremental form of the force-displacement relation incorporates the relaxation behavior of the viscoelastic material.

For oblique impacts between the spheres, shear forces are created in addition to the normal forces. The shear force-displacement relations for this work are based on Amonton's law of friction (Coulomb friction):

$$F^S = -\text{sgn}\left(v_{rel}^t\right)\mu\left|F^N\right| \tag{6}$$

where μ represents the coefficient of friction and v_{rel}^t is the relative tangential velocity. This simple model generally performs well. However, problems can arise with this model when the slip rate is small, as the shear force can rapidly change directions and create oscillations. Haff and Werner [14] proposed including a "viscous friction" term in the formulation. This term prevents the possibility of large force oscillations, but requires the need to define a shear damping coefficient which artificially adds damping to the system. Mindlin and Deresiewicz [15] studied the shear forces and determined that the shear force-displacement relations require a detailed set of equations depending on whether the normal and shear forces are increasing, decreasing, or remaining constant.

The alternative relations considered introduced additional problems or greater complexity without significantly improving the accuracy of the shear force-displacement relations. As a result, shear forces are currently calculated using Amonton's law of friction. The shear force-displacement relations will be modified if large force oscillations are observed during the simulations. A single coefficient of friction is given for particle-particle and particle-cavity contact. A kinetic coefficient of friction is given; i.e., it is assumed that particle motion occurs or that the static coefficient of friction is zero. The magnitude of the shear forces is based solely on the magnitude of the normal force and the coefficient of friction. The direction of the shear force opposes the relative tangential velocity between the contact surfaces. Relative tangential velocities can result from oblique impacts or due to rotation of the particles.

When particles collide with the cavity walls, particle-cavity force-displacement relations are required. The particle-cavity relations have been formulated by modifying the particle-particle relations to account for the material properties of the cavity and the local curvature. For example, particle-cavity relations for flat cavity walls are derived from the particle-particle relations by assuming the radius of curvature for the cavity goes to infinity. For simplicity, initially it has been assumed that the cavity walls are flat and rigid.

The background of the particle damper simulation code is based on X3D, an explicit finite element code typically used for impact analyses [16]. The code contains various contact algorithms and bookkeeping routines and provides an appropriate framework for simulating particle damping through the use of the particle dynamics method. Particle-particle and particle-cavity contacts are resolved using the force-displacement relations discussed in the preceding paragraphs. Figure 3 shows selected frames from a particle damper simulation with 64 steel spheres. The particles are initially given a random distribution within the cavity and include a gravity load which ensures that the particles pack on the bottom of the cavity. Further details on the modeling technique are discussed in the following section along with corresponding experimental test results.
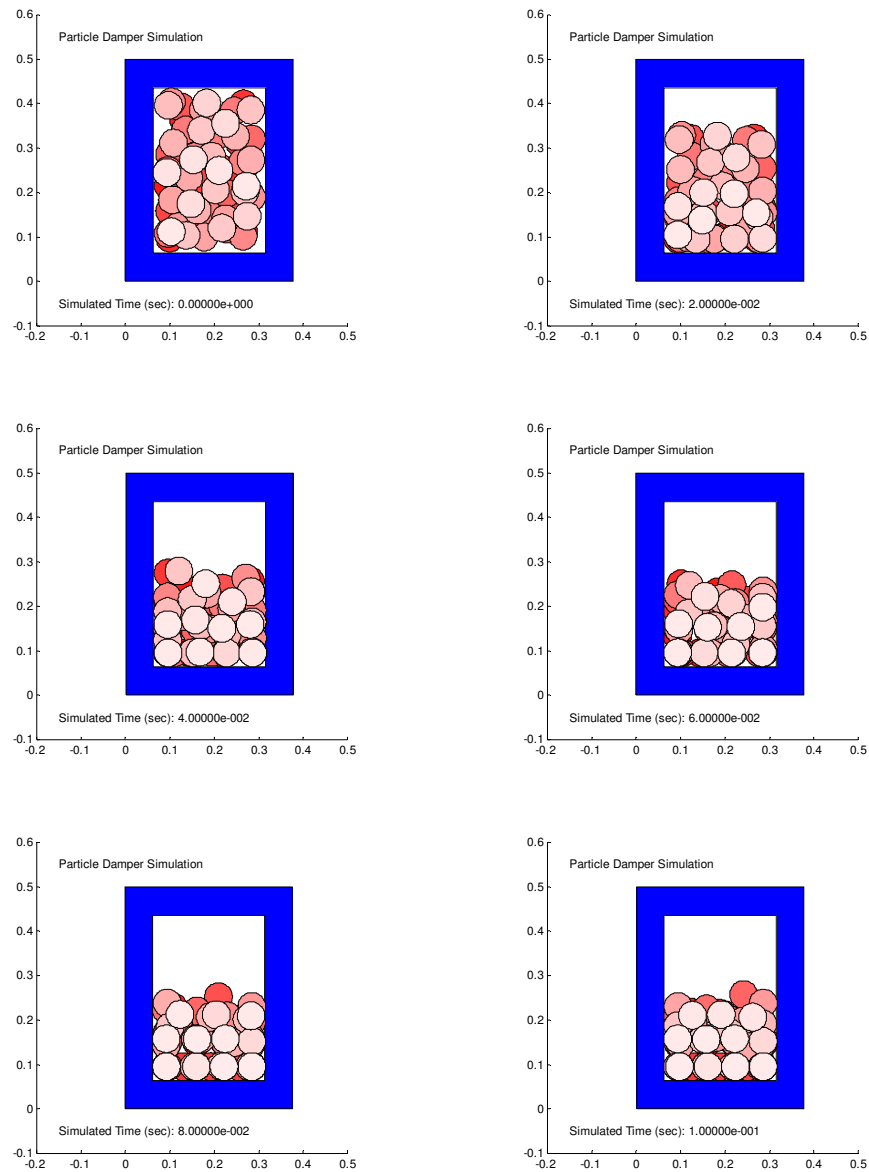

Figure 3: Selected frames from particle damper simulation

3. EXPERIMENTAL TEST METHODS

Preliminary experimental testing has been performed at room temperature using the test setup shown in Figure 4. A cantilevered aluminum beam is used as the test article. The first bending mode of the beam is excited harmonically near the root of the beam through a nylon stinger attached to a 50 pound shaker. Accelerations at the tip of the beam are measured

using an accelerometer and used to calculate the beam tip displacements. The particle dampers are placed near the tip of the beam where the largest displacements are observed for the first bending mode.
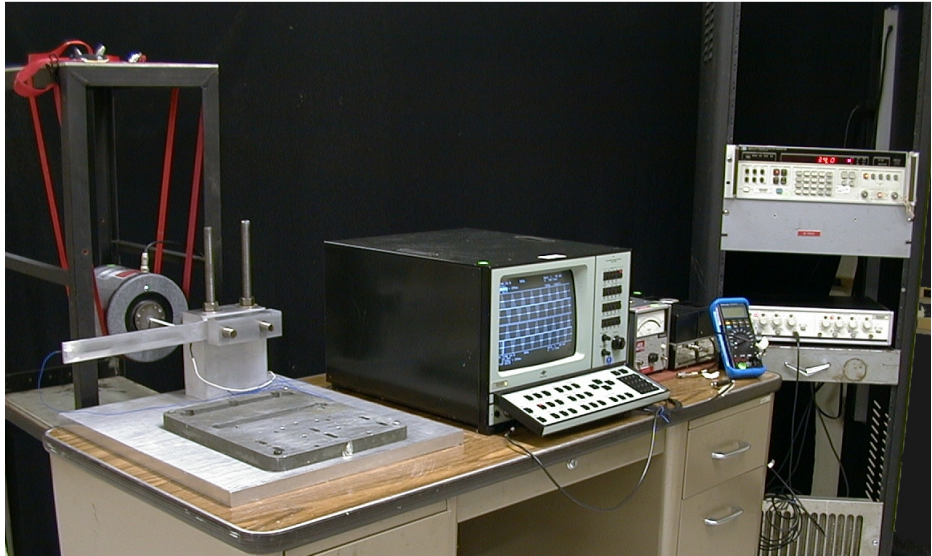

Figure 4: Experimental test setup

Preliminary analytical predictions have been made using a version of the X3D code modified for particle damper simulations. The aluminum beam used for the experimental testing is modeled as a simple mass-spring-dashpot system as shown in Figure 5. The beam has been modeled using a lumped mass (at the master cavity node) attached to a damped spring-to-ground element. The mass, spring stiffness, and damping are chosen to simulate the undamped beam. The beam system is excited by a prescribed sinusoidal force applied at the master cavity node. The cavity is modeled using contact surfaces defined by nodes which are linked to the master cavity node. Particles are tracked using a node at the center of each particle.
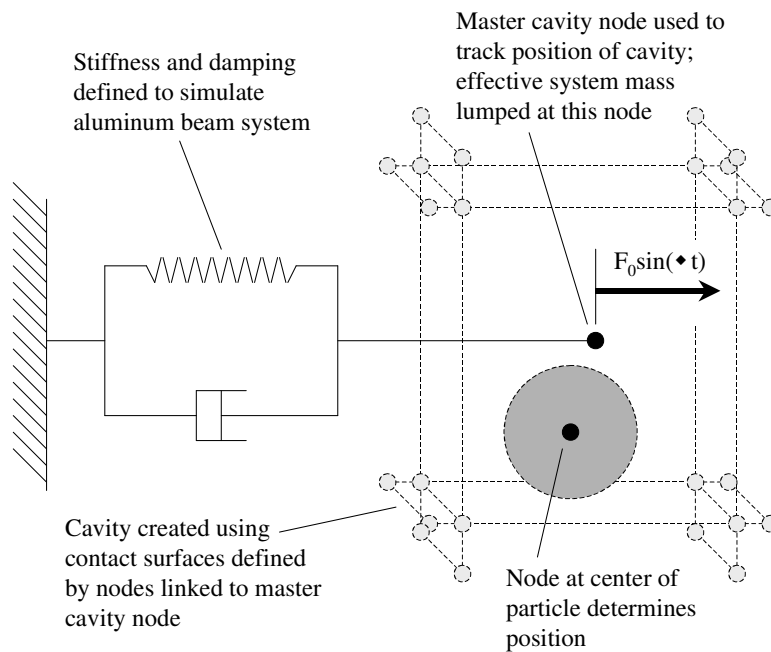

Figure 5: X3D model used to simulate impact and particle dampers

Figure 6 shows experimental and analytical results for the undamped aluminum beam and for the beam with particle dampers containing a single 0.250 inch diameter steel sphere with a clearance of 0.005 inch and with the single steel sphere replaced

with (64) 0.0625 inch diameter steel spheres. Predicted results for the beam with an added mass identical to that of the two dampers also are included. Two sets of results are given for the damper containing (64) 0.0625 inch diameter steel spheres. The first set of results (from ss003a) was taken with the excitation frequency increasing and the second set (ss004a) with the excitation frequency decreasing. Differences between these two results indicate that friction may significantly affect the damper behavior and illustrate some of the complex behavior which may occur with particle dampers. The analytical results shown in Figure 6 do not include friction. Additional particle damping simulations are being performed, along with continued experimental testing.
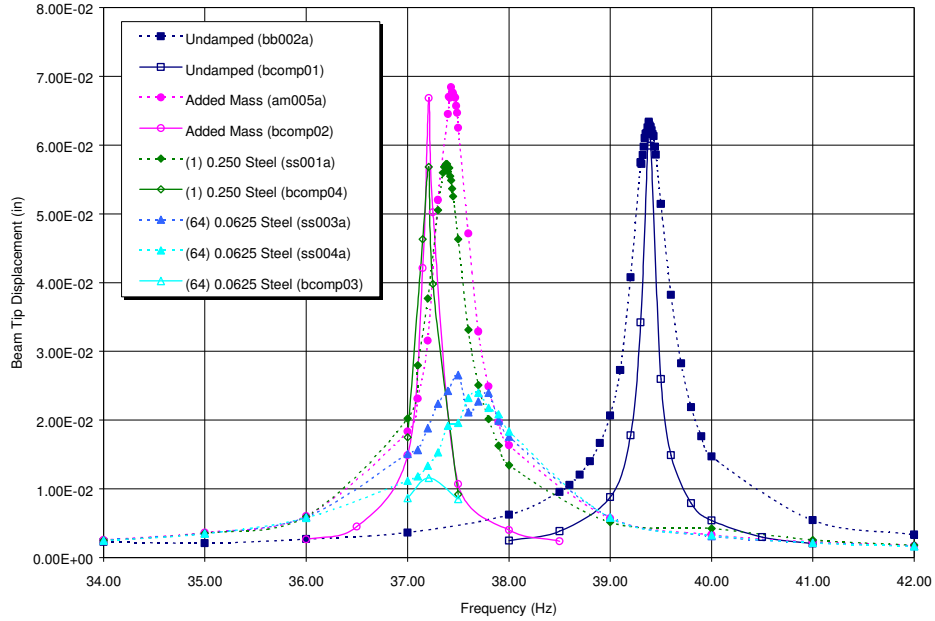

Figure 6: Comparison of preliminary experimental and analytical results

Additional experimental testing has been performed using a similar setup except with transient excitation. Analytical simulations of this testing have not been performed. By measuring the sinusoidal ring down of the structure, the damping can be calculated from the slope of the ring down envelope without measuring the input excitation. Assume that:

$$x(t) = Ae^{-\zeta\omega t}\cos(\omega t) \tag{7}$$

Take the Hilbert transform

$$H(t) = x(t) + jAe^{-\zeta\omega t}\sin(\omega t) \tag{8}$$

Take the absolute value

$$|H(t)| = Ae^{-\zeta\omega t} \tag{9}$$

Plot on a dB basis

$$\begin{aligned} dB &= 20\log\left(Ae^{-\zeta\omega t}\right) \\ &= 20\log A + (20\log e)(-\zeta\omega t) \end{aligned} \tag{10}$$

Rewrite, choosing $B = 20\log A / t$

$$\zeta = \frac{-(dB/t - B)}{(20\log e)\omega} = \frac{-(dB/t - B)}{(2\pi 20\log e)f} \tag{11}$$

Finally, consider the slope of the curve

$$\zeta = -(\text{slope in dB})/(54.6f) \tag{12}$$

Ring down data and Hilbert transform curve fit for an undamped beam is shown in Figure 7. Selected ring down measurements for multiple particles are shown in Figure 8 through Figure 10. It has been established that particle damping may be dependent on amplitude [4]. The change in slope of the curve fit shows the change in damping as the amplitude decreases. Figure 9 shows $\zeta = 0.0041$ for 80 particles at high amplitude. Figure 10 shows $\zeta = 0.0069$ within the same test at lower amplitude. Table 1 shows some of the test configurations examined.

Table 1. Preliminary ring down test configurations

Cavity	Particle size (dia. cm.)	Material	N Particles	Total mass (gms)
Equiv. mass			0 (equiv. mass)	1.2253
1.12776D x 1.27L	0.635	SS-302	1	1.0539
1.12776D x 1.27L	0.555625	SS-302	2	1.4121
1.12776D x 1.27L	0.47625	SS-302	3	1.3339
1.12776D x 1.27L	0.396875	SS-302	5	1.2865
1.12776D x 1.27L	0.3175	SS-302	10	1.3174
1.12776D x 1.27L	0.238125	SS-302	24	1.3338
1.12776D x 1.27L	0.15875	SS-302	80	1.3174
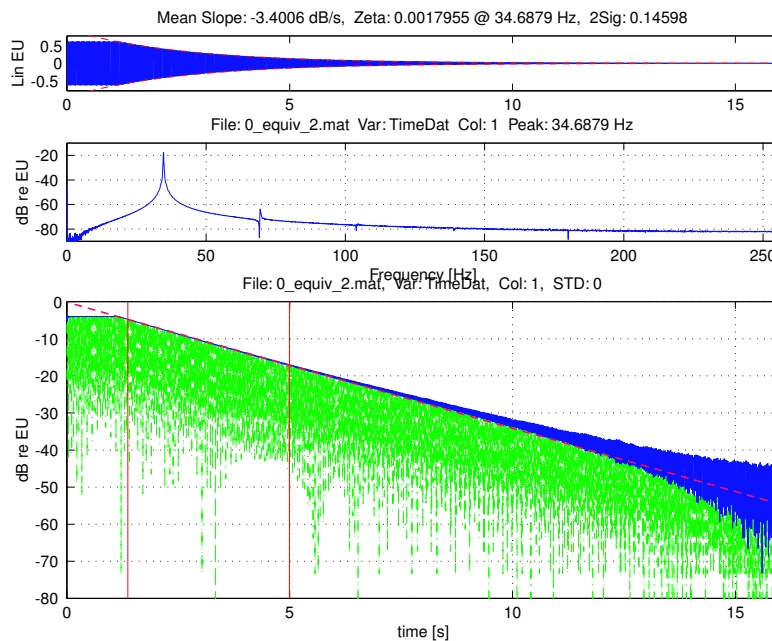
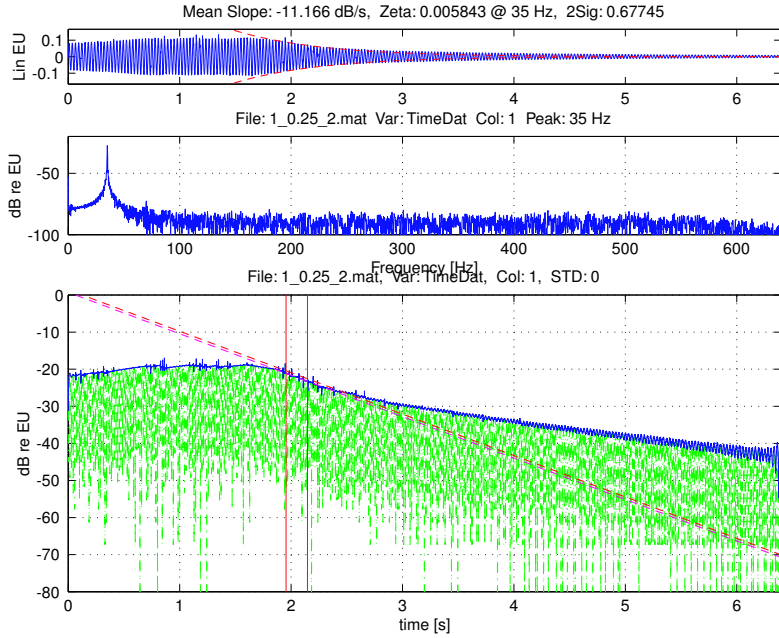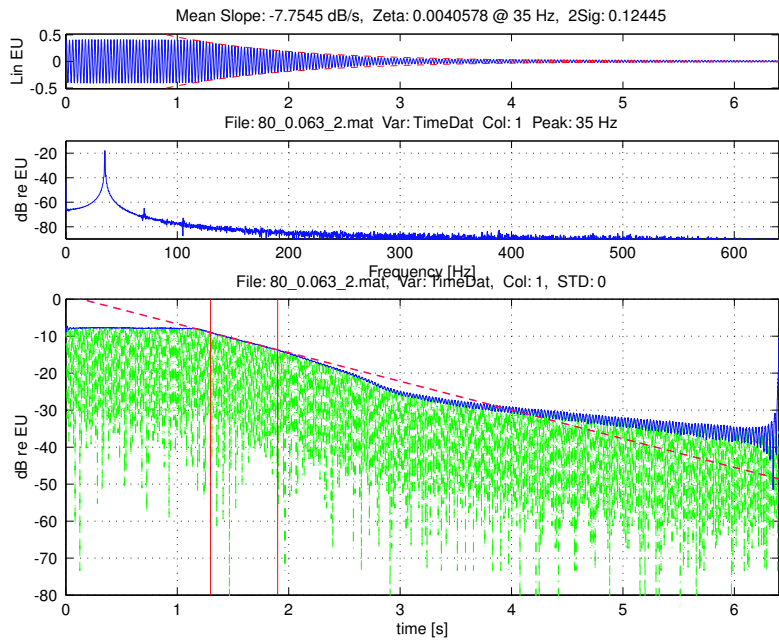Figure 7: Curve fit of Hilbert transform for beam with zero particles

Mean Slope: -11.166 dB/s, Zeta: 0.005843 @ 35 Hz, 2Sig: 0.67745

File: 1_0.25_2.mat Var: TimeDat Col: 1 Peak: 35 Hz

File: 1_0.25_2.mat, Var: TimeDat, Col: 1, STD: 0

Figure 8: One particle

Mean Slope: -7.7545 dB/s, Zeta: 0.0040578 @ 35 Hz, 2Sig: 0.12445

File: 80_0.063_2.mat Var: TimeDat Col: 1 Peak: 35 Hz

File: 80_0.063_2.mat, Var: TimeDat, Col: 1, STD: 0
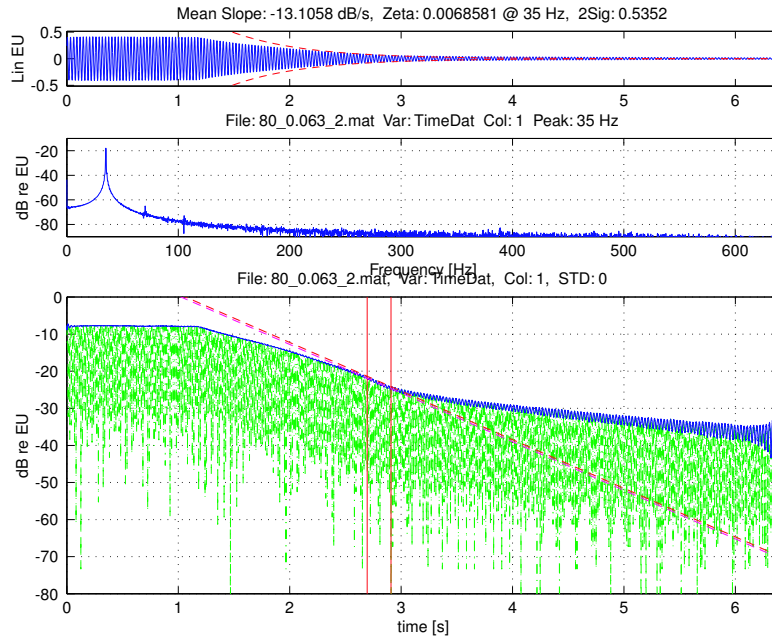
Figure 9: Eighty particles

Figure 10: Eighty particles, second damping measure

4. PARTICLE DAMPING UNDER CENTRIFUGAL LOAD

Particle damping is of interest as a possible damping mechanism for applications where high centrifugal loads exist such as the fan, compressor and turbines of aircraft engines. In these applications current design trends are removing traditional sources of damping such as frictional platform dampers in favor of the cost, weight, and performance efficiencies associated with integrally bladed disks and rotors.

Several critical questions exist with regards to the effectiveness of particle damping under centrifugal loads. The key question is will particle be able to move at all under realistic loads which can exceed 10,000 G's at locations where particle damping treatments would be likely to be integrated into a blade. While some researchers have seen damping with single particles under centrifugal loads (Flint [17], Duffy, *et al* [18-19]), others (Kielb [20]) have only seen limited effectiveness. Closer inspection of the test procedures has revealed that the actual achieved disturbance excitation levels and the ratio of these excitation levels to the centrifugal load levels are less than that which would be expected in a real blade and full rated speed.

In order to help remove the uncertainty associated with the low excitation levels a new centrifugal test facility is under development. Pictures of some of the hardware being developed for this new facility are shown in Figure 11. It will be capable of exposing the candidate damping treatments to centrifugal loads between 400 to 75,000 in a vacuum environment with out of plane disturbances between 0 to 200 G's using piezoelectric patches.
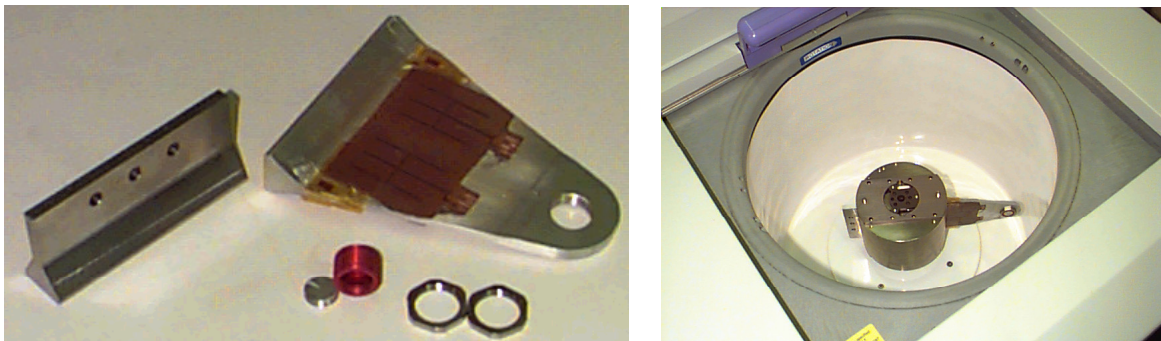

Figure 11: Test blade and other hardware during assembly and centrifuge fit checks

In an effort to pre-screen particle types in preparation for centrifugal testing, measurements of damping seen during ring down events for different particle combinations have been compared. Example measurements from test setups similar to

those already discussed are shown in Figure 12. The curves correspond to the floating average local damping of the ring down. Representative results are shown for non-damped baseline case, a single particle impact dominated case, and a multiple particle dominated case. The results are shown relative to 1 G. Note how both damping treatments return to the non damped performance once the disturbance level drops below a certain key value (approx. – 7 dB or .5 G) and how they have peak performance in different regions. These and similar results will be helpful in designing and interpreting the results of centrifugally loaded particle damping treatments when the test facility becomes operational in April 2000.
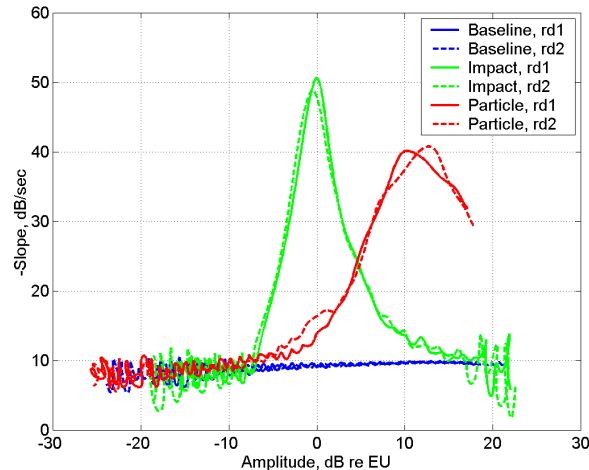

Figure 12: Comparison of time dependent damping extracted from ring down measurements

5. CONCLUSIONS

Preliminary experimental damping measurements have been made for a cantilevered beam system incorporating particle damping. Results from this testing demonstrate some of the challenges in predicting the highly nonlinear behavior of particle dampers, as parameters such as friction and excitation amplitude can significantly affect the behavior. An analytical model to predict particle damping has been developed. Correlation between preliminary experimental and analytical results is encouraging. Efforts are continuing, with work on real aerospace structures to be undertaken shortly.

6. AKNOWLEDGEMENTS

7. REFERENCES

1. Araki, Y., I. Yokomichi, and J. Inoue, "Impact Dampers with Granular Materials (2nd Report, Both Sides Impact in a Vertical Oscillating System)," *Bulletin of the Japanese Society of Mechanical Engineers*, Vol. 28, No. 241, p. 1466-1472, July 1985.
2. Yokomichi, I., Y. Araki, Y. Jinnouchi, and J. Inoue, "Impact Dampers with Granular Materials for Multibody System," *Journal of Pressure Vessel Technology*, Vol. 118, p. 95-103, February 1996.
3. Papalou, A., "Analytical and Experimental Studies of Impact Dampers," Ph.D. Dissertation for University of Southern California Civil Engineering Department, 1993.
4. Papalou, A., and S.F. Masri, "Response of Impact Dampers with Granular Materials Under Random Excitation," *Earthquake Engineering and Structural Dynamics*, Vol. 25, p. 253-267, 1996.
5. Papalou, A., and S.F. Masri, "An Experimental Investigation of Particle Dampers Under Harmonic Excitation," *Journal of Vibration and Control*, Vol. 4, p. 361-379, 1998.
6. Salueña, C., T. Pöschel, and S.E. Esipov, "Dissipative Properties of Granular Materials," *Physical Review E*, Vol. 59, No. 4, p. 4422-4425, April 1999.
7. Cundall, P.A., and O.D.L. Strack, "A Discrete Numerical Model for Granular Assemblies," *Geotechnique*, Vol. 29, No. 1, p. 47-65, 1979.

8. Cundall, P.A., and O.D.L. Strack, "The Development of Constituitive Laws for Soil Using the Distinct Element Method," Proceedings of the Third International Conference on Numerical Methods in Geomechanics, Aachen, April 2-6, 1979.
9. Cundall, P.A., A. Drescher, and O.D.L. Strack, "Numerical Experiments on Granular Assemblies: Measurements and Observations," Proceedings of the IUTAM Conference on Deformation and Failure of Granular Materials, Delft, August 31 – September 3, 1982.
10. Cundall, P.A., and O.D.L. Strack, "Modeling of Microscopic Mechanisms in Granular Material," Mechanics of Granular Materials: New Models and Constituitive Relations, J.T. Jenkins and M. Satake, eds., 1983.
11. Lee, E.H., and J.R.M. Radok, "The Contact Problem for Viscoelastic Bodies," *Transactions of the American Society of Mechanical Engineers*, Vol. 82, *Journal of Applied Mechanics*, Vol. 27, p. 438-444, 1960.
12. Ting, T.C.T., "The Contact Stresses Between a Rigid Indenter and a Viscoelastic Half-Space," *Transactions of the American Society of Mechanical Engineers*, Vol. 88, *Journal of Applied Mechanics*, Vol. 33, p. 845-854, 1966.
13. Ting, T.C.T., "Contact Problems in the Linear Theory of Viscoelasticity," *Transactions of the American Society of Mechanical Engineers*, Vol. 90, *Journal of Applied Mechanics*, Vol. 35, p. 248-254, 1968.
14. Haff, P.K., and B.T. Werner, "Computer Simulation of the Mechanical Sorting of Grains," *Powder Technology*, Vol. 48, p. 239-245, 1986.
15. Mindlin, R.D., and H. Deresiewicz, "Elastic Spheres in Contact Under Varying Oblique Forces," *Transactions of the American Society of Mechanical Engineers*, Vol. 75, *Journal of Applied Mechanics*, Vol. 20, p. 327-344, 1953.
16. Brockman, R.A., and T.W. Held, "X3D User's Manual," UDR-TR-92-59, University of Dayton Research Institute, Dayton, OH, 1994.
17. Flint, E., "Experimental Measurements of Particle Damping Effectiveness Under Centrifugal Loads", Proceedings of the 4[tjh] National Turbine Engine High Cycle Fatigue Conference Monterey, California, February 9-11, 1999.
18. Duffy, K., Brown, G., Mehmed, O., "Impact Damping of Rotating Cantilever Plates", Proceedings of the 3rd National Turbine Engine High Cycle Fatigue Conference, San Antonio, Texas, February 2-5, 1998.
19. Duffy, K., Bagley, R., Mehmed, O., "A Self-Tuning Impact Damper for Rotating Blades", Proceedings of the 4[tjh] National Turbine Engine High Cycle Fatigue Conference Monterey, California, February 9-11, 1999.
20. Kielb, R., *et al*., "Advanced Damping Systems for Fan and Compressor Blisks", Proceedings of the 4[tjh] National Turbine Engine High Cycle Fatigue Conference Monterey, California, February 9-11, 1999.